Neuropharmacology 105 (2016) 487–499

Contents lists available at ScienceDirect

Neuropharmacology

journal homepage: www.elsevier.com/locate/neuropharm

(I) Pharmacological profiling of a novel modulator of the α7 nicotinic receptor: Blockade of a toxic acetylcholinesterase-derived peptide increased in Alzheimer brains

Sara Garcia-Ratés*, Paul Morrill, Henry Tu, Gwenael Pottiez, Antoine-Scott Badin, Cristina Tormo-Garcia, Catherine Heffner, Clive W. Coen [1], Susan A. Greenfield

Neuro-Bio Ltd, Building F5, Culham Science Centre, Oxfordshire, OX14 3DB, United Kingdom

ARTICLE INFO

Article history:
Received 9 October 2015
Received in revised form
1 February 2016
Accepted 5 February 2016
Available online 8 February 2016

Keywords:
Acetylcholinesterase C-terminal peptide
Alzheimer's disease
α7nicotinic receptor
Cyclic peptide
Pheochromocytoma cells 12

ABSTRACT

The primary cause of Alzheimer's disease is unlikely to be the much studied markers amyloid beta or tau. Their widespread distribution throughout the brain does not account for the specific identity and deep subcortical location of the primarily vulnerable neurons. Moreover an unusual and intriguing feature of these neurons is that, despite their diverse transmitters, they all contain acetylcholinesterase. Here we show for the first time that (1) a peptide derived from acetylcholinesterase, with independent trophic functions that turn toxic in maturity, is significantly raised in the Alzheimer midbrain and cerebrospinal fluid; (2) a synthetic version of this peptide enhances calcium influx and eventual production of amyloid beta and tau phosphorylation via an allosteric site on the α7 nicotinic receptor; (3) a synthetic cyclic version of this peptide is neuroprotective against the toxicity not only of its linear counterpart but also of amyloid beta, thereby opening up the prospect of a novel therapeutic approach.

1. Introduction

There is still no effective treatment for neurodegenerative disorders such as Alzheimer's disease (AD), despite extensive research. Much effort has been directed towards targeting the histopathological markers amyloid beta (Aβ) and phosphorylated tau. However, a convincing account of the aetiology of AD should explain three basic questions that neither the Aβ (Morris et al., 2014) nor the tau (Gendron and Petrucelli, 2009) hypothesis can fully address. First, why does Alzheimer's frequently co-occur with another degenerative disorder, Parkinson's disease (Horvath et al., 2014)? Second, given that amyloid precursor protein (APP) is widespread in the brain (Card et al., 1988), why are only specific neurons lost in the initial stages of AD (Aletrino et al., 1992; Braak and Del Tredici, 2011)? Third, why is this loss initially in the 'global neuron' groups (Woolf, 1996) within the basal forebrain, midbrain and brainstem that degenerate in AD or Parkinson's disease (PD) or in both diseases (Aletrino et al., 1992; Braak and Del Tredici, 2011)?

A common feature of these primarily vulnerable 'global neurons' is the conspicuous presence of acetylcholinesterase (AChE) co-localised *not* with its cognate substrate acetylcholine (ACh), but with diverse, unrelated transmitters (Albanese and Butcher, 1980). Hence, as has long been acknowledged (Greenfield, 2013), AChE is likely to have an alternative, non-enzymatic role in these particular nuclei.

We have consequently proposed (Greenfield, 2013) that this non-enzymatic role could involve a peptide that has a conspicuous sequence homology to amyloid beta (Aβ) (Fig. 1A), but is derived from the carboxy-terminus of AChE (AChE-peptide). Our earlier work has shown that it is bioactive in a range of tissues, including rat hippocampal organotypic cultures (Day and Greenfield, 2004), as well as *ex vivo* brain slices from guinea-pig (Bon and Greenfield, 2003) and rat hippocampus (Greenfield et al., 2004) or prefrontal cortex (Badin et al., 2013). The peptide enhances calcium entry (Bon and Greenfield, 2003), can modulate plasticity (ie LTP) (Greenfield et al., 2004) and may act as a developmental signalling molecule (Greenfield, 2013).

Evidence that this peptide exists as an independent entity is suggested by the prevalence in embryonic and early postnatal development of a monomeric form of AChE (G1) (Arendt et al., 1992; Garcia-Ayllon et al., 2010) from which the AChE-peptide

* Corresponding author. Tel.: +44 (0)1235 420085.
E-mail address: sara.garciarates@neuro-bio.com (S. Garcia-Ratés).
[1] School of Medicine, King's College London, London, United Kingdom.

http://dx.doi.org/10.1016/j.neuropharm.2016.02.006
0028-3908/

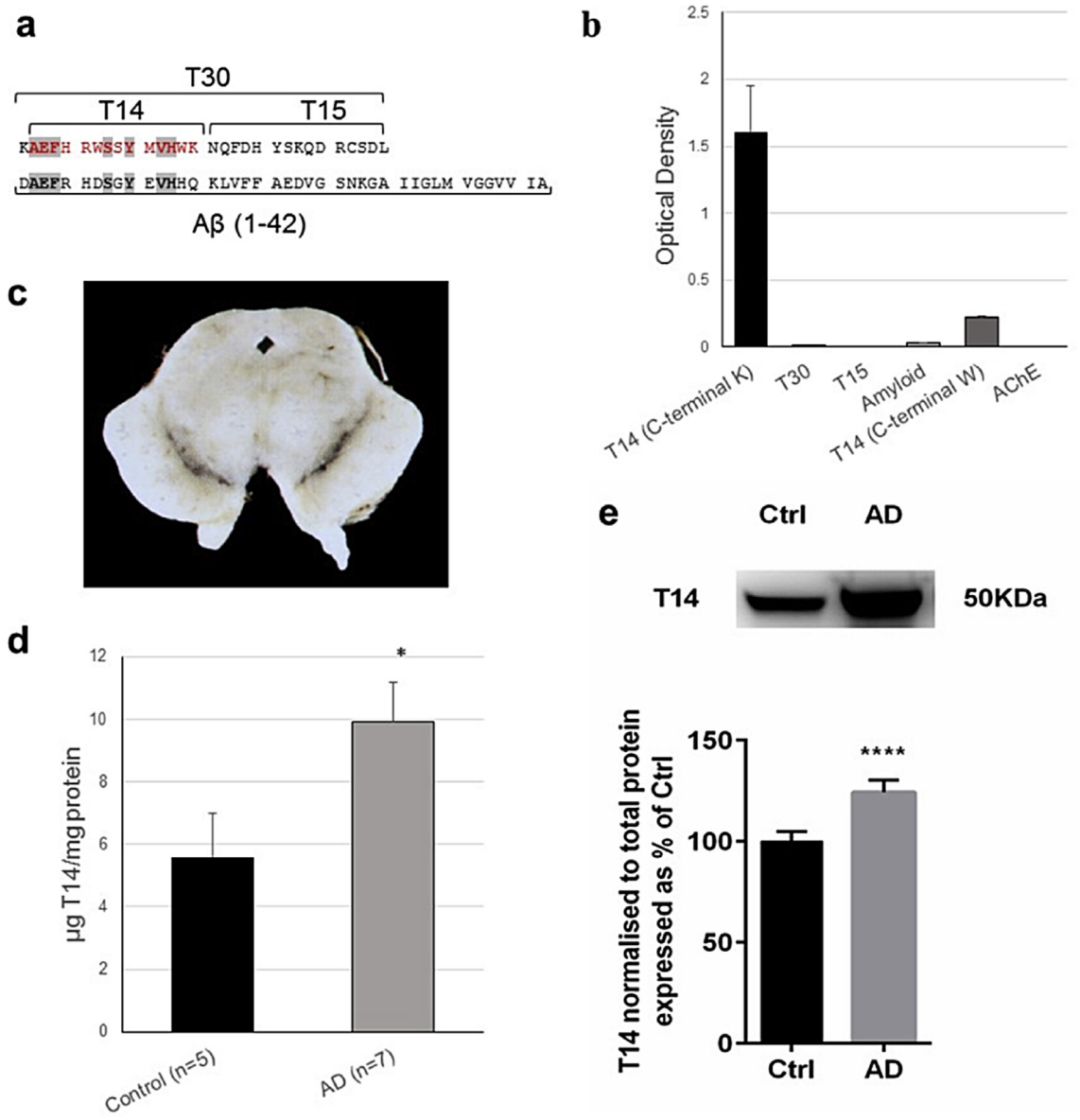

Fig. 1. A peptide fragment derived from AChE is higher in AD. 1a: Sequence alignment of Aβ (1–42) with T30 peptide: T14 (red) and residual T15. Amino acids common to both sequences are shaded. 1b: Mean ± SEM immunoreactivity to 100 nM T14, T30, T15, Aβ, T14 without the C-terminal K residue or AChE. 1c: Midbrain tissue block representative of those used in this study. This section incorporates the 'global neurons' first described by Woolf (Woolf, 1996) and implicated in the initiation of neurodegenerative disorders (Rossor 1981; Greenfield 2013)as well as production of Aβ (Irwin et al., 2013). 1d: Mean ± SEM immunoreactivity in control (n = 5) and AD midbrains (n = 7). Levels expressed as µg T14 peptide per mg protein in brain homogenate. Significant difference at level $P < 0.05$ indicated by *. 1e top panel: T14 immunoreactivity in post-mortem CSF from controls (Ctrl) and AD patients in a representative Western blot. Due to aggregation (Bond et al., 2009; Cottingham et al., 2002), T14 shows an electrophoretic band at 50 KDa. Ctrl: Male, 80 y/o, CERAD normal, Braak I. AD: Male, 81 y/o, CERAD definite, Braak V. 1e bottom panel: Quantification of T14 immunoreactivity in post-mortem CSF of Ctrl (n = 10) and AD patients (n = 10). T14 levels were normalised to total protein as detected by Blot-Faststain™ (Collins et al., 2015) and expressed as percentage of the average of controls ± SEM. Significant difference at level $P < 0.0001$ indicated by ****.

has been cleaved at the C-terminus; consequently the parent molecule is unable to oligomerise and the liberated peptide is available to perform independent actions (Bond et al., 2009; Cottingham et al., 2002). Its initially beneficial trophic action of triggering calcium influx in development (Bon and Greenfield, 2003; Greenfield et al., 2004) could turn toxic in maturity (Garcia-Rates et al., 2013; Greenfield, 2013), as suggested by the increased abundance of the residual molecule G1 in AD (Garcia-Ayllon et al., 2011). In the case of the adult brain, where tolerance to calcium influx is much lower (Eimerl and Schramm, 1994), the erstwhile trophic actions can shift to one of calcium-mediated excitotoxicity (Dickie et al., 1996) via an allosteric site on the α7 nicotinic receptor (Greenfield et al., 2004). Hence the initiating process for the neurodegeneration may be an aberrant recapitulation of development (Greenfield, 2013).

The first aim of this study was to test this hypothesis. We investigated whether AChE-peptide can be detected in human brain tissue, and whether there are differences in its concentration in the brainstem (midbrain) and cerebrospinal fluid (CSF) between age-matched controls and AD patients.

The second aim was to determine whether *in vitro* application of synthetic AChE-peptide leads to a constellation of biochemical features that may be indicative of AD, e.g. calcium-triggered activation of glycogen-synthase-kinase-3 (GSK-3) (Hartigan and

Johnson, 1999) leading to production of Aβ, at the expense of its parent APP, and phosphorylation of tau (Hartigan and Johnson, 1999).

The third aim was to see whether these established features of AD pathology, as well as further toxic effects of both AChE-peptide and Aβ (calcium influx, cell viability, compensatory AChE release) (Garcia-Rates et al., 2013), can be prevented by intercepting the binding of AChE-peptide (Greenfield et al., 2004) to an allosteric site on the α7 nicotinic receptor. Accordingly, we synthesised the cyclic variant of AChE-peptide that was anticipated to display enhanced stability (Goodwin et al., 2012) relative to its linear counterpart (Howell et al., 2014), and to act as an antagonist (Lamberto et al., 2014).

2. Results

2.1. A novel peptide increased in Alzheimer's brain

Although the bioactive component of the AChE-peptide is contained within a 14 amino acid sequence (T14, Fig 1a), it has been administered in previous and current experiments as part of a larger molecule of 30 amino acids (T30) (Bond et al., 2009). The T30 peptide is less likely to form fibrils and is therefore more stable in solution and thus more effective than the smaller T14 (Bond et al., 2009; Cottingham et al., 2002). For present purposes, an antibody was raised against the T14 peptide (the active part of the C-terminal AChE). This antibody was tested against T14 and a range of additional compounds serving as controls: Aβ, the full length T30 sequence, a peptide (T15) consisting of the inert C-terminal 15 amino acid residues of T30 (Fig 1a) (Bond et al., 2009) and AChE. The antibody shows a strong affinity for T14, but does not recognise Aβ, T30, T15 or AChE; moreover, there is substantially reduced immunoreactivity to a variant of synthetic T14 lacking the final lysine residue and ending with tryptophan (C-terminal W) (Fig 1b). These observations indicate that the antibody binds to this terminal region of T14 and that this region is conformationally inaccessible to the antibody in T30 or AChE.

Homogenates of human midbrain (Fig 1c) passed through a filter eliminating compounds higher than 30 KDa (e.g. proteins such as AChE itself) showed immunoreactivity to the antibody that had been raised against the synthetic AChE-peptide T14. The amount of T14 immunoreactivity detectable was significantly ($p = 0.0327$) higher in samples from Alzheimer brains compared with age-matched controls (Fig 1d). Note that none of the AD brain tissue tested here was from patients who also displayed PD-like symptoms. Significantly elevated levels of T14 were also detected in CSF from AD patients compared with age-matched controls using Western Blotting ($p < 0.0001$, Fig. 1e).

2.2. AChE-peptide triggers Alzheimer-like effects

PC12 cells are derived from a pheochromocytoma of the adrenal medulla with an embryological provenance from the neural crest; they have been described as a 'window on the brain', and can display the histological markers of both AD and PD diseases (Appleyard and McDonald, 1991; Takeda et al., 1994; Bornstein et al., 2012). Such cell lines offer a unique means of exploring not only normal physiological processes, but also pathological mechanisms (He et al., 2010; Garcia-Ayllón et al., 2014). Accordingly, the potentially pathological effects of T30 and Aβ were tested in this system. When T30 (5 μM) was introduced for 48 h to PC12 cells, there was an increase in phosphorylated GSK-3 of 52.6 ± 6.93% above control ($p < 0.01$, $n = 4$, Fig. 2a), a decrease in membrane APP to 69.74 ± 7.1% of control ($p < 0.05$, $n = 4$, Fig 2b), an increase in Aβ release of 40.47 ± 13.14% above control ($p < 0.05$, $n = 8$, Fig. 2c) and a 24.14 ± 1.21% increase above control in phosphorylated tau ($p < 0.01$, $n = 4$, Fig 2d). In parallel studies on each of these parameters, T15 was used as a control for non-specific peptide effects and did not induce any effect on GSK-3 activation, APP, Aβ or tau phosphorylation.

We then compared the toxicity of AChE-derived peptides with that of Aβ, and explored whether their effects may be differentiated from the non-specific actions of H_2O_2 (Eckert et al., 2005). Accordingly, we tested all four treatments (T30, T14, Aβ, H_2O_2) on a trio of parameters previously shown (Garcia-Ayllon et al., 2010) to give rise to a pathological profile in PC12 cells: (1) immediate calcium influx, (2) compromised cell viability an hour later accompanied by (3) 'compensatory' AChE release (Garcia-Ayllon et al., 2010), as suggested by the significant negative correlation ($R = -0.550$, $p < 0.05$) of the latter two concomitant parameters. The effects of T30 and T14 peptides (5 μM) were compared with those of the same concentration of Aβ and an equipotent toxic concentration of H_2O_2 (100 μM): all induced calcium influx (Fig. 3d), T30 and T14 being significantly ($p < 0.05$) more potent (171.05 ± 16.8%) than Aβ (121.18 ± 13.52%) and H_2O_2 (137 ± 15.2%, $n = 10$). All four treatments significantly ($p < 0.01$) compromised cell viability (Fig. 3e) (T30: 74.3 ± 2.16%; T14: 80.0 ± 5.76%; Aβ: 78.2 ± 3.67%; H_2O_2: 73.9 ± 3.63%, $n = 10$). A significant ($p < 0.01$) compensatory enhancement of AChE release was observed following Aβ (124.19 ± 3.91%, $n = 10$) and T14 (132.83 ± 1.74%, $n = 10$); this was significantly ($p < 0.001$) higher following T30 (169.45 ± 3.87%, $p < 0.001$, $n = 10$). No change was seen following the non-specific toxin H_2O_2.

2.3. A novel blocking agent: NBP14

The cyclisation of the peptide T14 was achieved by coupling the N-terminal alanine to the C-terminal lysine (see methods) to give the novel cyclic peptide 'NBP14' (Fig. 3a, b). In contrast to the linear T14, the cyclised version was immunonegative to the T14 antibody, as were the other control peptides (Fig. 1b). Moreover, unlike its linear counterpart, NBP14 applied on its own (0.5 μM) proved to have no significant effects in the following tests: Aβ (89.78 ± 6.54% of control), APP (101.87 ± 3.75% of control) or phosphorylation of GSK-3 (104.32 ± 0.1% of control) or tau (87.96 ± 6.9% of control). Similarly, no effect was seen on cell viability (104.36 ± 2.70% of control), on calcium influx (96.29 ± 3.1% control) or on AChE release (105.415 ± 3.26% of control).

However, when NBP14 was applied with T30, it abolished the actions of T30 in generating the AD-like profile, namely the activation of GSK-3 (returning to 95.52 ± 0.755% of control), decrease of APP (returning to 95.12 ± 10.77% of control), increase of Aβ (returning to 97.48 ± 5.14% of control) and phosphorylation of tau (returning to 103.85 ± 11.77% of control). Furthermore, NBP14 was neuroprotective in all three measures of the toxic actions of T30 or T14: calcium influx (96.29 ± 3.1% & 79.8 ± 16.4%), cell viability (98.63 ± 3.81% & 103.86 ± 12.5%) and AChE release (105.4 ± 3.26% & 112.3 ± 1.39%). NBP14 also inhibited the actions of Aβ: calcium influx (93.79 ± 2.8%), cell viability (95.10 ± 4.63%), and AChE release (102.63% ± 2.7%).

NBP14 returned the T30 or T14 enhancement of ACh-primed calcium influx to the control level (representative trace for T30, Fig. 3c; $p < 0.01$ for T30 and T14, $n = 10$, Fig. 3d), as was the case for the influx induced by Aβ ($p < 0.05$, $n = 10$, Fig. 3d). In addition, the decrease in cell viability observed on treatment with Aβ, T30 or T14 was completely prevented by NBP14 ($p < 0.01$, $n = 10$, Fig. 3e). Finally, the marked increase in AChE release following T30 or T14 application was abolished by NBP14 ($p < 0.001$ for T30 and T14, $n = 10$, Fig. 3f), as was the case for the increase seen with Aβ application ($p < 0.01$, $n = 10$, Fig. 3f).

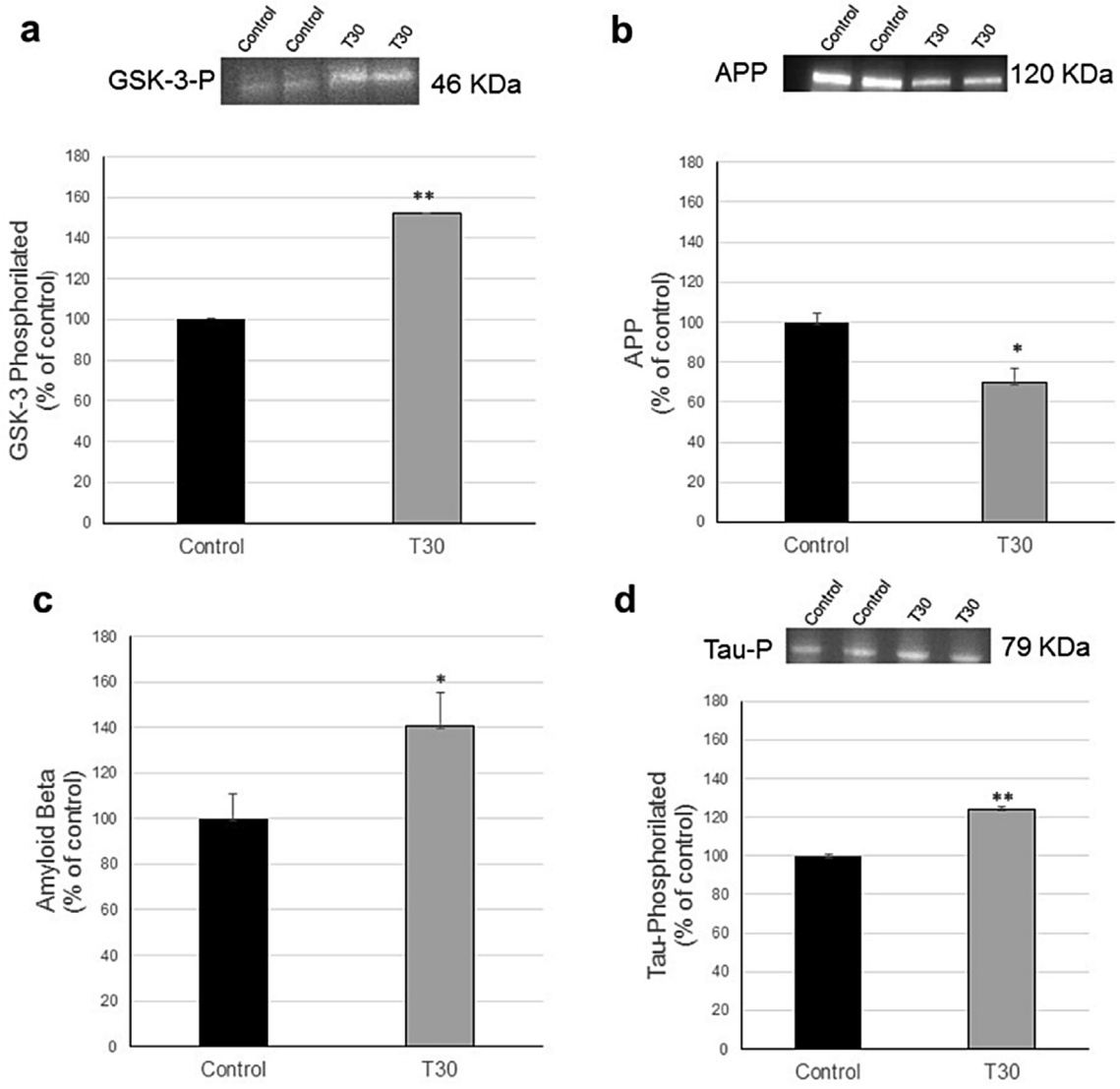

Fig. 2. AChE-peptide T30 can induce an Alzheimer-like profile. The effects of AChE-peptide (T30, 5 μM) on four parameters that are affected in AD. T30 significantly (2a) enhances phosphorylation of GSK-3, (2b) decreases membrane APP, (2c) increases Aβ release and (2d) increases phosphorylated tau. Significant differences at level $p < 0.05$ indicated by * and $p < 0.01$ indicated by **. Note that although detection of secreted Aβ was possible by ELISA as shown, the protein concentration available in the medium was too low to be charged in a gel for Western blots, unlike the 3 other parameters that were membrane bound.

2.4. Comparison of NBP14 efficacy with galantamine

NBP14 (2 μM) showed no anti-AChE activity. This is in contrast to the strong inhibitory effect seen with galantamine, an established drug in clinical use for AD with various pharmacological effects including action at the alpha-7 nicotinic receptor (Samochocki et al., 2000) (Fig 4a).

Another marked difference was observed between NBP14 and galantamine when the binding of the two agents was compared in displacing ivermectin, a positive modulator at an allosteric site of the α7 nicotinic receptor, that potentiates the calcium influx initially induced by a primary agonist such as ACh or choline. Whilst, in PC12 cells, galantamine showed an IC50 of 57.1 μM with only partial displacement of ivermectin, NBP14 was some 50 times more potent at 1.1 μM (Fig. 4b and c) with complete displacement. In contrast to galantamine, NBP14 showed no binding to the nicotinic α4β2 receptor (data not shown). A similarly stronger binding of NBP14 over galantamine was shown in membranes isolated from rat brain (Fig 4d), where the IC50 for galantamine was lower than in PC12 cells. This difference is probably due to the admixture of other receptors in the rat membrane preparation, suggesting multiple targets for galantamine but not for NBP14, for which the values in the membrane preparation (IC50 1.79 μM) and in the cell line (IC50 1.1 μM) remained similar.

A final comparison was made of the neuroprotective effects of NBP14 and galantamine (Table 1, n = 10). The minimum concentration needed for NBP14 to protect against the deleterious effects on cell viability of either T30 or Aβ was, in both cases, 500 pM. In contrast, galantamine showed protection against T30 starting at 5 nM (i.e. 10 times less effective than NBP14) compared with protection against Aβ at 100 nM (i.e. 200 times less effective than NBP14).

3. Discussion

The independent presence of a C-terminal peptide fragment derived from AChE has been previously inferred (Garcia-Rates et al., 2013; Greenfield, 2013) from the existence in the brain of the

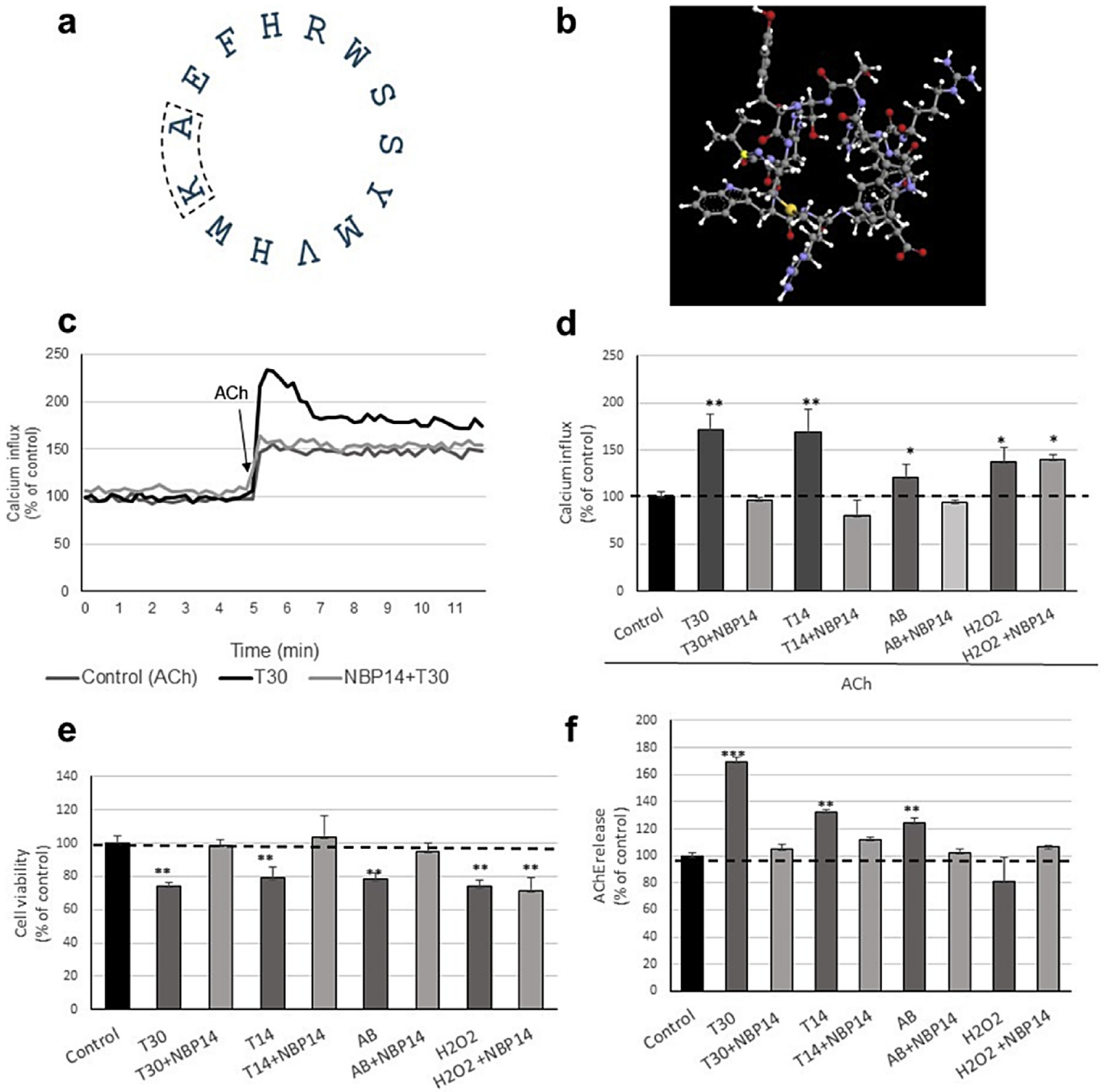

Fig. 3. The effects of AChE-peptides T30 & T14 compared with Aβ and H_2O_2 on PC12 cells and their reversal by NBP14. 3a: Cyclisation of T14 peptide (Fig. 1a), NBP14. 3b: Molecular model of NBP14. 3c: Representative traces of ACh-primed (100 μM) calcium influx enhanced by T30 (5 μM) and reversed in the presence of NBP14 (0.5 μM). 3d: The effects on calcium influx after application of T30 (5 μM), T14 (5 μM), Aβ (5 μM), H_2O_2 (100 μM) either alone or in the presence of NBP14 (0.5 μM). 3e: T30, T14, Aβ (5 μM) and H_2O_2 (100 μM) compromise cell viability; NBP14 (0.5 μM) prevents this response for only T30, T14 or Aβ. 3f: 'Compensatory' release of AChE occurring at the same time as cell viability is compromised by T30, T14, or Aβ (5 μM) is completely blocked by NBP14 (0.5 μM). Significant differences $p < 0.05$ indicated by * and $p < 0.01$ indicated by **.

monomer G1 of AChE (Arendt et al., 1992; Garcia-Ayllon et al., 2010) where oligomerisation via disulphide bond formation is not possible due to the absence of the C-terminal AChE-peptide. Although such circumstantial evidence suggested that the AChE-peptide exists as an independent biochemical entity, this is the first study showing its presence in brain tissue using an antibody against the bioactive 14 amino acid sequence (T14) within the AChE-peptide T30 (Bond et al., 2009). The antibody used here does not recognise the following: Aβ, the whole AChE molecule, T30, the inert 15 amino acid sequence (T15) at the C-terminus of T30 or T14 lacking its terminal lysine. These results indicate that the antibody binds to this terminal region of T14 and that this region is conformationally inaccessible to the antibody in T30 or in the whole AChE molecule. The present study has detected immunoreactivity for T14 in the brain and CSF; the level is shown to be doubled in the AD midbrain, a site incorporating the 'global neurons' (Woolf, 1996) in which neurodegeneration appears to originate (Braak and Del Tredici, 2011) and increased by 24% in post-mortem CSF samples

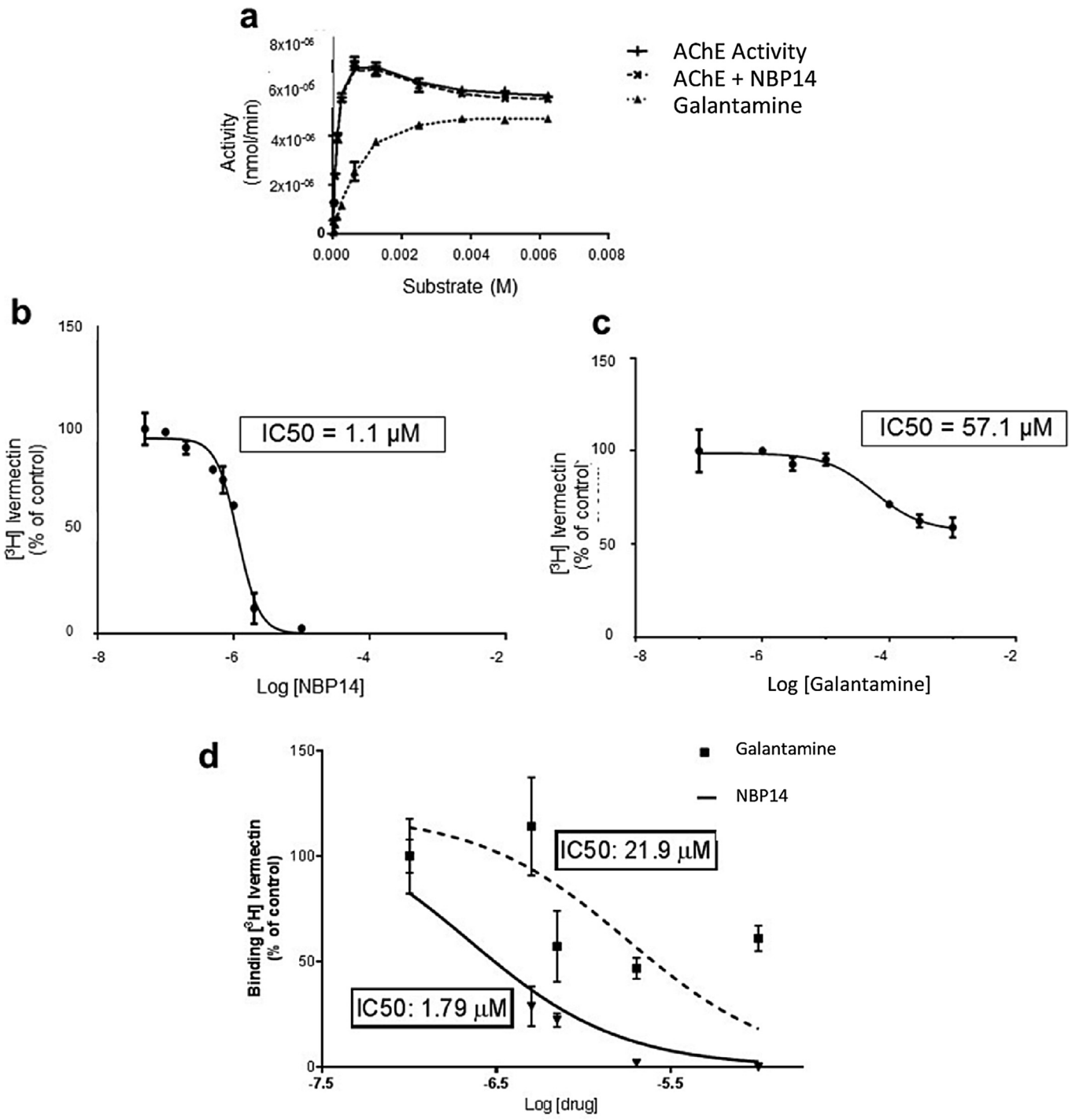

Fig. 4. Comparison of NBP14 with galantamine. 4a: Activity-substrate relations for exogenous AChE alone and in the presence of either galantamine or NBP14 (2 μM). Whilst NBP14 has no effect on enzyme activity, galantamine is strongly inhibitory, reducing activity of AChE by some 50%. 4b and 4c: Comparison between NBP14 and galantamine of displacement of radiolabelled ivermectin, a selective a7 receptor allosteric ligand, in PC12 cells. Note NBP14 binds with an affinity 50 times greater than galantamine with an IC50 of 1.1 μM and 57.1 μM 4d: Comparison between NBP14 and galantamine of displacement of radiolabelled ivermectin, a selective a7 receptor allosteric ligand, in rat brain membranes. Note NBP14 binds with an affinity 20 times greater than galantamine with an IC50 of 1.79 μM and 21.9 μM.

from AD patients.

Aβ, abnormally cleaved from APP, has long been linked to the pathogenesis of AD; but impeding its synthesis has not yet proved to be an effective strategy for therapy (Mondragon-Rodriguez et al., 2012). As was pointed out some 30 years ago, the virtual ubiquity of APP in the brain must mean that 'the susceptible cell populations have unique properties' (Card et al., 1988; Darvesh, 2013). We suggest that the key, permissive factor may be the presence of increased AChE-peptide. There has been much controversy as to whether Aβ or phosphorylated tau are the primary agents driving the neurodegenerative process (Giacobini and Gold, 2013). However, since, as shown here, T30 leads to increases in both Aβ and tau phosphorylation, it is plausible that such effects in the aetiology of AD are downstream consequences of the initial actions of the AChE-

Table 1
Comparison of neuroprotective effects of NBP14 versus galantamine.

Cell viability (% of Control)			Cell viability (% of Control)		
Treatment	% Average	% SEM	Treatment	% Average	% SEM
NBP14 5 pM + T30	76.55**	2.26	Gal 5 pM + T30	73.07**	3.88
NBP14 50 pM + T30	80.86*	5.32	Gal 50 pM + T30	77.40**	5.03
NBP14 100 pM + T30	82.47*	6.86	Gal 100 pM + T30	83.02*	7.50
NBP14 500 pM + T30	**83.42**	**8.27**	Gal 500 pM + T30	83.36*	7.59
NBP14 1 nM + T30	**92.49**	**4.31**	Gal 1 nM + T30	83.58*	6.53
NBP14 5 nM + T30	**94.30**	**2.29**	Gal 5 nM + T30	**91.30**	**6.02**
NBP14 10 nM + T30	**95.23**	**6.59**	Gal 10 nM + T30	**91.96**	**5.55**
NBP14 50 nM + T30	**94.30**	**3.50**	Gal 50 nM + T30	**91.88**	**9.46**
NBP14 100 nM + T30	**94.89**	**4.46**	Gal 100 nM + T30	**90.23**	**7.02**
NBP14 500 nM + T30	**98.63**	**3.82**	Gal 500 nM + T30	**93.39**	**5.14**
Cell viability (% of Control)			Cell viability (% of Control)		
Treatment	% Average	% SEM	Treatment	% Average	% SEM
NBP14 5 pM + AB	83.53**	1.43	Gal 5 pM + AB	83.06*	4.60
NBP14 50 pM + AB	80.50**	1.91	Gal 50 pM + AB	83.42*	6.39
NBP14 100 pM + AB	83.99*	2.69	Gal 100 pM + AB	85.19*	6.07
NBP14 500 pM + AB	**92.89**	**2.43**	Gal 500 pM + AB	82.20*	5.27
NBP14 1 nM + AB	**92.49**	**3.71**	Gal 1 nM + AB	81.56*	3.96
NBP14 5 nM + AB	**89.06**	**0.67**	Gal 5 nM + AB	83.21*	3.04
NBP14 10 nM + AB	**92.56**	**2.75**	Gal 10 nM + AB	85.83*	1.85
NBP14 50 nM + AB	**91.29**	**0.65**	Gal 50 nM + AB	85.55*	2.34
NBP14 100 nM + AB	**94.44**	**4.30**	Gal 100 nM + AB	**96.27**	**3.15**
NBP14 500 nM + AB	**100.02**	**3.09**	Gal 500 nM + AB	**94.50**	**1.64**

Comparative dose-responses of NBP14 and galantamine (Gal) against 5 μM T30 or 5 μM Aβ toxicity on cell viability. *vs Control $P < 0.05$, **vs Control $P < 0.01$ and ***vs Control $P < 0.001$.

peptide. Such a sequence may explain why neurodegeneration commences in certain populations of neurons (Card et al., 1988; Braak and Del Tredici, 2011). Aβ and phosphorylated tau may be widespread in the CNS; in contrast, the AChE-peptide appears to characterise the primarily vulnerable neurons (Greenfield, 2013).

Moreover, the case for the AChE-peptide being a candidate for primary driver in Alzheimer pathogenesis is enhanced by the discovery of its greater potency over Aβ in the range of tests used here. Aβ, T30, T14 and the non-specific toxic agent H_2O_2 (Eckert et al., 2005) were all found to compromise cell viability and potentiate calcium influx; however, only Aβ, T14 and T30 selectively triggered 'compensatory' AChE release.

The alpha-7 nicotinic receptor has been shown to be the receptor for amyloid has been previously shown to be alpha-7 (Wang et al., 2000), as also demonstrated electrophysiologically for the AChE-peptide in oocytes transfected with the alpha-7 receptor (Greenfield et al., 2004). PC 12 cells (as used here) do not possess any form of nicotinic receptor that triggers calcium entry other than alpha-7 (Rogers et al., 1992; Nery et al., 2010). Alpha-4 beta-2 nicotinic receptors are operational in these cells, but they are exclusively sodium ionophores (Rogers et al., 1992). Thus, the ACh-triggered calcium influx monitored here is mediated via alpha-7 receptors. Amyloid or the AChE-peptide influence calcium influx only in the presence of the primary ligand ACh (Fig. 3d); hence, they must be acting at a secondary, allosteric site. Furthermore, as reported here (Fig. 3d), the response elicited by each of these modulatory agents is blocked by NBP14 (itself inert), which binds to this receptor with high affinity (Fig 4d). Thus, the cell death and release of AChE, subsequent to the enhanced calcium entry, can only be attributed to an initial activation of the alpha 7 receptor acting as a calcium ionophore, enhanced by the modulatory action of either T30 or amyloid which in turn can be blocked by NBP14 occupying an allosteric site.

By introducing AChE-peptide into the pathological scenario (Fig 5), we may be able to explain where and how the neurodegenerative mechanism is set in train: the crucial factor is the role of the AChE-peptide as a characteristic and highly selective feature of the vulnerable cells, instigating a feed-forward mechanism for perpetuating excessive calcium entry through the alpha-7 nicotinic receptor (Bond et al., 2009).

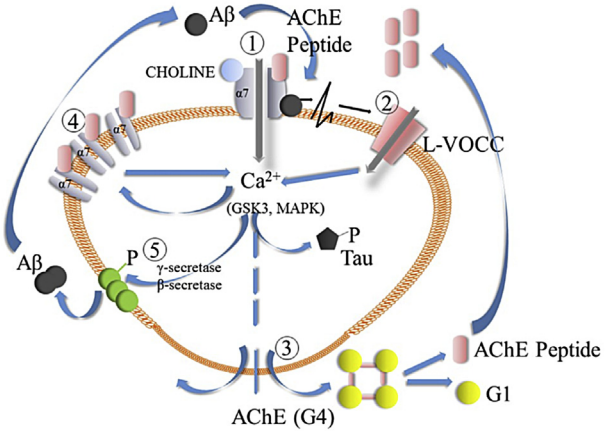

Fig. 5. Scheme of an intracellular cascade showing how AChE-peptide could instigate a feed-forward chain of pathological events. 1: AChE-peptide binds to α7 nicotinic receptor and enhances Ca^{2+} influx (Greenfield et al., 2004). Note that this action need not be restricted to cholinergic systems since ubiquitous dietary choline can act as an alternative primary ligand. 2: Depolarisation activates voltage-sensitive calcium channels (L-VOCC) (Dickinson et al., 2007). 3: Raised intracellular calcium induces increase in AChE G4 release (Greenfield, 2013). 4: Calcium triggers upregulation of the α7 nicotinic receptor causing more Ca^{2+} influx and generating still more targets for AChE-peptide (Bond et al., 2009). 5: Calcium activates the enzyme GSK-3 (Hartigan and Johnson, 1999) that will (a) increase tau phosphorylation and AChE release (Garcia-Ayllón et al., 2014) and (b) activate γ-secretase/β-secretase thereby releasing Aβ to act at the NBP14-sensitive site on α7 nicotinic receptors, as shown by the current data.

The parallels between AChE and Aβ can be readily listed: first, there is a striking sequence homology between Aβ and the part of the AChE-peptide (Fig 1a) that has been shown to be responsible for its non-enzymatic actions (Greenfield, 2013); second, Aβ enhances the expression of AChE in neurons and glia (Saez-Valero et al.,

2003); third, as shown here, the T30 AChE-peptide enhances the production of Aβ from APP, suggesting a synergy between the two agents; finally both Aβ (Ni et al., 2013) and AChE-peptide (Greenfield et al., 2004) act at the alpha-7 nicotinic receptor. Once the process of neurodegeneration is underway, both Aβ and AChE-peptide are likely to synergise by acting either at two sites on the same subunit or by cooperative binding to the same site on different subunits of the five identical ones available in the alpha-7 nicotinic receptor in a way that perpetuates further cell death by triggering the 'compensatory' release of AChE (Garcia-Rates et al., 2013), an effect that is positively correlated with the degree of cell death. In turn, the released AChE-peptide acts on the increasing numbers of alpha-7 nicotinic receptors (Bond et al., 2009) to induce more Aβ and *vice versa* (see Fig 5) We conclude that the AChE-peptide may be the primary trigger for AD and that interception of its action at the alpha-7 nicotinic receptor would be an attractive therapeutic goal.

The alpha-7 nicotinic receptor is distributed in a diverse range of cell types and has a calcium permeability even greater than the N-methyl-D-aspartate receptor (Seguela et al., 1993). As such it is not surprising that it has already been implicated in the pathological process: in the transgenic AD mouse there is elevated Aβ (Wang et al., 2000) that causes upregulation of the alpha-7 nicotinic receptor (Svedberg et al., 2002). Thus both receptor and ligand have been implicated in AD (Nagele et al., 2002). Moreover, this receptor proliferates in AD (Chu et al., 2005; Ni et al., 2013) and has long been linked to the actions of the AChE-peptide (Greenfield et al., 2004), not least as it is co-expressed within the same neuronal populations and time window as AChE in the developing brain (Broide et al., 1996).

The practice of cyclisation of compounds to improve their stability is not new (Gilon et al., 1991; Goodwin et al., 2012) and has been exploited previously as a therapeutic strategy (Haworth et al., 1999). However, to the best of our knowledge, cyclisation of a peptide to act as a blocker of its endogenous, linear counterpart in relation to neurodegenerative disorders is unprecedented. As shown here, NBP14 proved to be non-toxic when applied alone; however, the protective effect of NBP14 against T30 and Aβ is demonstrated for three parameters that are inter-linked, one being immediate (calcium influx) and the other two (cell viability and compensatory AChE release) being observed an hour later. Thus, the action of NBP14 at an allosteric site on the alpha-7 nicotinic receptor may have potential as a novel therapeutic strategy for halting the degenerative process. Moreover, current evidence suggests that NBP14 is active in the physiological environment of the *ex vivo* mammalian brain (Badin et al., 2016.)

Galantamine, an established drug currently used to target this receptor, has not proved to be effective in arresting the cell loss in AD, but only in slowing the progression of the disease in its early stages (Coyle and Kershaw, 2001). Moreover, galantamine is associated with a range of side effects due to its actions at the alpha-4 beta-2 nicotinic receptor (Samochocki et al., 2000), which is the second most abundant nicotinic receptor in the brain after the alpha-7 nicotinic receptor, and to its inhibitory effects on AChE (Coyle and Kershaw, 2001). In contrast, these constraints do not apply to NBP14, which neither binds to the alpha-4 beta-2 nicotinic receptor (data not shown), nor has any effect on AChE activity. Moreover, NBP14 is neuroprotective against the toxic actions of T30 and Aβ, with a 10–200 fold greater potency than galantamine depending on the insult.

The relative clinical inefficacy of galantamine may be because in the actual circumstances of AD and related disorders (as opposed to *in vitro* pharmacological preparations) a key allosteric site on the alpha-7 nicotinic receptor may be already occupied by T14, a naturally occurring high affinity binding molecule. In contrast, the more stable cyclic version of T14 could displace its linear counterpart more readily while being inactive *per se*. Whilst agents like galantamine, NS1738, CCMI, LY-2087101 and ivermectin act in the transmembrane region of the receptor and are positive allosteric modulators on their own (Ludwig et al., 2013), NBP14 appears to be unique in being intrinsically inert. In contrast to these positive allosteric modulators that potentiate calcium influx but have limited clinical efficacy, NBP14 abolishes the deleterious effects of both Aβ and the AChE-derived peptide by reducing excess calcium influx and thus potential excitotoxicity.

Transgenic models (Laurijssens et al., 2013; Laferla and Green, 2012) have proved to be useful for targeting aspects of the disease, such as amyloid, tau and inflammation, that may not be primary instigators, as proposed in the new scheme (Fig 5). The scenario proposed here would therefore require development of completely different transgenic models for further behavioural and pharmaceutical testing. Meanwhile, NBP14 and its actions, as shown here, are novel and may offer greater insight into the pharmaco-dynamics of the alpha-7 nicotinic receptor, as well as prompt the development of a therapy for arresting the continuing process of cell death that characterises AD and related neurodegenerative disorders.

4. Conclusions

In summary, this study provides:

- The first report of a novel biomarker, the peptide T14, detectable with a custom-made antibody, for which levels are significantly increased in AD brains and CSF.
- Evidence that the T14 peptide drives the production of amyloid and hyperphosphorylation of tau, i.e. replicating the profile of AD pathology.
- The first report of a novel alpha-7 allosteric compound that is inert (i.e. not a positive modulator) but neuroprotective against toxic agents in a cell line recognised as a good model for neurodegeration and in *ex vivo* brain slices (Badin et al., 2016).
- A novel mechanism for AD (Fig 5).

5. Methods

5.1. T14 antibody

The antibody was synthesised by Genosphere Biotechnologies (Paris, France). Two New Zealand rabbits were used with four immunisations with keyhole limpet hemocyanin (KLH)-peptide (T14-hapten: CAEFHRWSSYMVHWK; C was included to link to KHL as immunogen) over 70 days. The animals were bled four times and the bleeds pooled.

The antiserum was then passed through a gravity column with covalently bound peptide-support and, following washing, the antibodies were eluted in acidic buffer and the solution neutralised. Further dialysis against phosphate buffered saline (PBS) buffer and lyophilisation completed the process.

5.2. ELISA for T14 peptide antibody

The standard curves and the samples were run in triplicate. The human homogenate samples were diluted 1:160 (see below). The standard curve for determination of T14 peptide in brain tissue samples were diluted in PBS buffer. The standard curve ranged from 8 to 100 nM of T14. Briefly, 96-well immunoplates (NUNC) were coated with 100μl/well of sample or standard T14, covered with parafilm and incubated overnight at 4 °C. The following day the

sample was removed by flicking the plate over a sink with running water, and 200 μl of the blocking solution containing 2% bovine serum albumin (BSA) in Tris-buffered saline and Tween 20 (TBS-T) was added and incubated for 4 h at room temperature. Blocking solution was then removed and 100 μl of antibody, diluted in blocking solution to 1 μg/ml, was added and incubated overnight at 4 °C. The primary antibody was removed the next day and wells were washed 3 times with 200 μl of TBS-T. After 100 μl of secondary enzyme-conjugated antibody diluted in blocking solution to 0.1 μg/ml was added and incubated for 2 h at room temperature; the plate was covered with parafilm during all incubations. After 2 h, the plate was washed 4 times with TBS-T. The addition of 3,3,5,5-tetramethylbenzidine started the colour reaction. The reaction was stopped 30 min later with stopping solution containing 2 M H_2SO_4, and the absorbance was measured at 450 nm in a Vmax plate reader (Molecular Devices, Wokingham, UK).

5.3. Human clinical samples

Midbrain blocks of fresh-frozen tissue and cerebrospinal fluid were supplied by the Thomas Willis Oxford Brain Collection (c/o Professor Margaret Esiri). The blocks were approximately 5 mm in rostro-caudal extent, containing the dorsal raphe, substantia nigra, red nucleus, cerebral peduncles and third nerve nucleus. An ethics application was approved by the Human Tissue Bank of the Oxford Radcliffe Hospital NHS that complied with the Human Tissue Act, Human Tissue Authority Codes of Practice and other law relevant to *post mortem* examinations and use of tissue.

5.4. Preparation of human samples

The brain samples were prepared as follows: they were weighed before being placed in a dounce and 1.5 μL of PBS was added per 1 mg of brain material. The samples were homogenised by using the “loose” plunger. The “tight” plunger was used to further homogenise the material. The homogenised sample was collect in 2 mL Eppendorfs were centrifuged for 15 min at 13,000 g, 4 °C. Once the centrifugation was finished, the supernatant was collected into 0.5 ml 30 KDa MWCO filters. The samples were centrifuged for 30 min at 13,000 g and protease inhibitor cocktail (Roche complete PIC 04693116001) was added to the filtrate. This was used for the ELISA for T14 peptide. The unfiltered sample retentate (>30 kDa) was collected by reversing the filter into a separate microcentrifuge tube and was used to determine the concentration of protein of the initial sample using the Pierce assay (as described below). For the CSF, samples were unfiltered and used directly for electrophoresis.

5.5. Protein determination

The Thermo Scientific Pierce 660 nm Protein Assay is a ready-to-use, detergent- and reducing agent-compatible assay to quickly measure total protein concentration compared to a protein standard of bovine serum albumin. For the assay, 10 μl of each human brain homogenate sample (diluted 1:10 in PBS) were added to a microtiter 96 well-plate followed by the addition of 150 μl of Pierce assay. After 5 min incubation, the absorbance was measured at 660 nm in a Vmax plate reader (Molecular Devices, Wokingham, UK) and the results of optical density were extrapolated to the standard curve of BSA to obtain μg per μl.

5.6. PC12 cell cultures

PC12 cells are a cloned, pheochromocytoma cell line derived from the adrenal medulla (Greene and Tischler, 1976). They are easily cultured and readily accessible to experimental manipulations. Since chromaffin cells are derived from the neural crest but are located in the centre of an accessible peripheral organ (the adrenal medulla) they have been described as offering a ‘window’ into the brain (Bornstein et al., 2012). These cells serve as a powerful *in vitro* model for studying the still unknown primary process of neurodegeneration. The reasons why they are useful for the present project are as follows: the adrenal medulla in Alzheimer's patients shows various pathological features comparable to those seen in the central nervous system, e.g. numerous Lewy-body like inclusions, neurofibrillary tangles and paired helical filaments, as well as expression of APP (Takeda et al., 1994). PC12 cells were selected for this work because present the same features as chromaffin cells. Wild-type PC12 were purchased from Sigma–Aldrich (St. Louis, MO). The culture was routinely plated in 100 mm dishes (Corning) coated with collagen (2 μg/cm^2) and maintained in growth medium with Minimum Essential Medium Eagle (MEM) supplemented with heat-inactivated 10% horse serum (HS) and 5% foetal bovine serum (FBS), 10 mM 4-(2-hydroxyethyl)-1-piperazineethanesulfonic acid (HEPES), 2 mM L-Glutamine and 1:400 Penicillin/streptomycin solution. Cells were maintained at 37 °C in a humidified atmosphere 5% CO_2 and the medium was replaced every 2 days. For splitting, cells were dislodged from the dish using a pipette with medium, with a portion of these replated onto new culture dishes. Cells were used between passages 12 and 25.

5.7. Aβ preparation

Aβ (1–42) fibrils were prepared as described by the provider (Abcam, Cambridge UK). 1 mg of Aβ (1–42) was dissolved in 212 μl of 1 ml of 100% 1,1,1,3,3,3-hexafluoro-2-propanol (HFIP) and 10 μl of NH_4OH. This solution was incubated at room temperature for 1 h. Next, the solution was sonicated for 10 min and then after sonication and distribution of 10 μl of sample per tube, samples were dried in a speed vacuum drier (Thermo Fisher Scientific, Loughborough, UK) and stored at −80 °C. For experiments, samples were diluted in 20 μl of 100% dimethyl sulfoxide (DMSO) and incubated for 2 h at room temperature (5 mM) and 98 μl of HCl (0.01 M) to ensure fibril formation and incubated over night at 37 °C.

5.8. NBP14 synthesis

NBP14 was synthesised by Genosphere Biotechnologies (Paris, France). First they synthesised the linear T14 peptide and afterward they proceed with the cyclisation. Three techniques were used to achieve cyclisation of linear peptides described, i.e. sidechain-to-sidechain, sidechain-to-backbone, and head-to-tail cyclisation. Head-to-tail cyclisation has been investigated extensively, and can involve directed Cys–Cys disulphide cyclisation (up to two per molecule). Careful monitoring of the reaction ensures 100% cyclisation. Two general approaches are used for synthesis: (1) classical solution-phase linear peptide cyclisation under high dilution conditions; and (2) resin-based cyclisation. Two distinct successful protocols were employed in the solid phase synthesis. Resultant samples of cyclic peptides were analysed by MALDI-TOF MS.

5.9. NBP-14 design by Argus lab

The NBP-14 was designed *in silico* by using the free software Argus lab. The molecule was built by using the option Polypeptide builder and the best conformation of the structure was optimized by using a geometry optimization parameter, Hamiltonian UFF, in a maximum of 100,000 steps.

5.10. Cell viability assay

A Cell Counting Kit-8 (CCK-8) was used. By utilising the highly water-soluble tetrazolium salt (WST-8), CCK-8 produces a water-soluble formazan dye upon reduction in the presence of an electron carrier. WST-8 is reduced by dehydrogenases in cells to give a yellow coloured product (formazan), which is soluble in the tissue culture medium. The amount of the formazan dye generated by the activity of dehydrogenases in cells is directly proportional to the number of living cells. PC12 cells were plated in 200 μl of complete growth medium the day before the experiment in 96 well plates. Treatments with T30, T14 or Aβ alone or in conjunction with NBP14 or galantamine at different concentrations were added and incubated for 1 h in the incubator. Subsequently, 100 μl of growth medium were removed and 10 μl of CCK-8 solution were added. The plate was incubated for 2 h in the incubator and then placed in the absorbance plate reader. The absorbance was measured at 450 nm in a Vmax plate reader (Molecular Devices, Wokingham, UK).

5.11. AChE activity assay

AChE activity was measured using the Ellman reagent that measures the presence of thiol groups as a result of AChE activity. In the case of the G4 experiment, AChE (G4) activity was tested alone and also together with either NBP14 or galantamine. For the PC12 experiment, cells were plated the day before the experiment as for the cell viability assay. Cells were treated with T30, T14 or Aβ (5 μM) alone or combined with NBP14 (0.5 μM). After treatment, supernatant (perfusate) of each treatment was collected and 25 μL from each condition were added to a new flat bottomed 96 well plate followed by the addition of 175 μl of Ellman reagent (Solution A: KH_2PO_4 139 mM and K_2HPO_4 79.66 mM, pH 7.0; solution B (substrate): Acetylthiocholine Iodide 11.5 mM; Solution C (Reagent): 5, 5'-dithiobis (2-nitrobenzoic acid) 8 mM and $NaHCO_3$ 15 mM). The Ellman reagent was prepared as a mixture of the 3 solutions in a ratio 33(A):3(B):4(C). Absorbance measurements were taken for an interval of 60 min across experiments at 405 nm in a Vmax plate reader (Molecular devices, Wokingham, UK).

5.12. Calcium fluorometry

PC12 cells were plated in 200 μl of Dulbecco's Modified Eagle's medium (DMEM) plus 2 mM of L-glutamine medium the day before the experiment in 96 well plates. On the day of the experiment, the Fluo-8 solution (Abcam) was prepared as described by the provider by adding 20 μl of Fluo-8 in the assay buffer that contains 9 ml of Hank's Balanced Salt Solution (HBSS) and 1 ml of pluronic F127 Plus. Subsequently, 100 μl of growth medium was removed and 100 μl of Fluo-8 solution were added. Treatments with T30, T14 or Aβ in conjunction with NBP14 were added and incubated for 30 min in the incubator and 30 min room temperature. After 1 h, the plate was placed in the fluorescence plate reader (Fluostar, Optima, BMG Labtech, Ortenberg, Germany). Before reading the fluorescence, acetylcholine (ACh) 100 μM, an agonist of the nicotinic receptors, was prepared and placed in the Fluostar injector. For each well, the reading was formed by a basal fluorescence reading followed by acetylcholine injection that induced an increase of calcium via nicotinic receptors.

5.13. Cell membrane preparation

PC12 membranes where obtained to perform binding assays. PC12 cells were grown until confluence on 100 mm plates. Growth medium was removed and ice-cold 50 mM Tris–HCl buffer (pH 7.4) containing 4.5 μg/μl aprotinin and 0.1 mM phenylmethylsulphonylfluoride (PMSF) and phosphatase inhibitor cocktail were added. Cells were mechanically split and pelleted by centrifugation (1040 × g) for 4 min at 4 °C. Pellets were homogenised with a Polytron and centrifuged (13,000 × g) for 20 min at 4 °C. The pellets were resuspended in fresh buffer and incubated at 37 °C for 10 min to remove endogenous neurotransmitters. The samples were subsequently re-centrifuged. The final pellet was resuspended in buffer and the protein concentration determined using the Thermo Fisher Pierce Assay 660 nm. The cell membrane preparation was stored at −20 °C.

5.14. Rat brain membrane preparation

Brains from P40 Wistar male rats (Charles River) were obtained and homogenised with a Polytron in a sucrose buffer: 320 mM sucrose, 5 mM Tris–HCl and protease inhibitors (aprotinin 4.5 μg/μl + pMSF 0.1 mM + orthovanadate 1 mM; pH 7.4). The volume of buffer was calculated as 10 ml buffer per gram of brain. Then the samples were centrifuged for 30 min, at 4 °C, 15,000 × g. The pellet was resuspended and the samples were centrifuged (×2) for 30 min at 15,000 g and resuspended in Tris–HCl 50 mM plus the aforementioned mixture of protease inhibitors. The protein concentration was determined by Pierce Assay.

5.15. [^{3}H] Ivermectin binding assay

For the binding with PC12 membranes and rat brain membranes, each incubation was performed in polystyrene tube (VWR International Ltd; Leicestershire, UK) containing 0.25 ml of membranes diluted in Tris–HCl 50 mM buffer (containing 50 μg of PC12 membranes or 200 μg of rat brain membranes) with 5 nM [^{3}H] ivermectin (American Radiolabeled Chemicals, USA) in the absence or presence of different concentrations of NBP14 or galantamine (0.1, 0.5, 0.7, 1, 2, 10, 100, 1000 μM) diluted in Tris–HCl 50 mM, in a final volume of 0.5 ml for 2 h at 4 °C. Thereafter, samples were filtered through Brandel GB glass fibre filters (MD, USA); presoaked in 0.5% polyethylenemine by a Harvester (Brandel; MD, USA). Tubes were washed 3 times with ice cold 50 mM Tris–HCl buffer. Radioactivity in the tubes was counted by scintillation spectrometry using a 300SL Liquid scintillation counter (Lablogic Systems Limited, UK). Specific binding was determined by subtracting the non-specific (cells treated with ivermectin 30 μM) value to all the tubes. Moreover, to discard the binding of ivermectin to purinergic receptors present in PC12 cells, ATP was added to the membranes resulting in no binding.

5.16. Solubilisation of protein

PC12 cells were plated with growth medium in Petri dishes for a week in order to have enough protein to detect APP, GSK-3, tau and Aβ in PC12 cells and treated for 1 h or 48 h with T30, T15 or NBP14, depending on the experiment, before solubilising the protein. For the Aβ ELISA, the medium of the cells was used. Once the cells had grown until 90% confluence, the growth medium was removed and kept for ELISA and cells were re-suspended in 2 ml of HBSS. The cells suspension was transferred to a 15 ml tube and centrifuge 5 min at 1000 rpm. Then the supernatant was discarded and the pellet was re-suspended in lysis buffer (20 mM Tris, 137 mM NaCl, 1% Triton X-100, 2 mM EDTA; pH 8) plus protease inhibitors (1 μl: 1 ml phenylmethylsulfonyl fluoride (PMSF), 1 μl: 1 ml phosphatase cocktail-3 and 3 μl: 1 ml aprotinin) and triturated by using a Polytron for 10 s. Subsequently, the triturated pellet was distributed in 1.5 ml Eppendorfs and rotated or shaken for 2 h at 4 °C. After 2 h, the Eppendorfs were centrifuged at 13,000 rpm for 20 min and the supernatant was kept for Western Blot. The Bradford reagent is

used to quantify the protein contained in each Eppendorf.

5.17. Electrophoresis and Western Blot

A general Western blot and immunodetection protocol was used to determine the levels of APP, phosphorylated GSK-3, phosphorylated tau and T14. PC12 cells were cultured onto 92 mm plates and treated with either T30 (5 μM), T15 (5 μM), NBP14 (0.5 μM), NBP14 + T15 or NBP14 + T30 for 48 h. Then the cells were washed with ice-cold phosphate buffer, split and collected from the plate, pelleted by low-speed centrifugation, and solubilised in lysis buffer (20 mM Tris–HCl pH 8, 137 mM NaCl, 2 mM ethylenediaminetetraacetic acid (EDTA), and 1% nonidet P-40) by incubation for 2 h at 4 °C under gentle shake. Thereafter, the samples were centrifuged at 13,000 × g for 20 min at 4 °C, and the supernatants containing solubilised proteins were stored at −20 °C, after determination of protein content using the Thermo Scientific Pierce 660 nm Protein Assay (explained above). For each sample, 10 μg of protein (20 μg for CSF samples) was mixed with sample buffer (0.5 M Tris–HCl, pH 6.8, 10% glycerol, 2% (w/v) sodium dodecyl sulphate, 5% (v/v) 2-β-mercaptoethanol, 0.05% bromophenol blue, final concentrations), boiled for 10 min, and loaded onto a 10% acrylamide gel. Proteins were separated by electrophoresis until the elution of the migration front to allow proper separation of high molecular weight fragments. Proteins were then transferred from gels to polyvinylidene fluoride sheets (Thermo Fisher). These sheets were blocked for 1 h at room temperature with 5% defatted milk in Tris-buffered saline buffer plus 0.05% Tween 20 (TBS-T buffer). They were then incubated overnight with a rabbit monoclonal antibody against APP (ab2072, Abcam, Cambridge, UK; dilution 1:1000), or phospho-GSK-3 (Tyr279/Tyr216) (05-413, Millipore, Hertfordshire, UK; dilution 1:1000) or phosphorylated tau (MN1020, Thermo Fisher, Northumberland, UK; 1:1000) or T14 antibody (1:1000, Genosphere), diluted in TBS-T buffer plus 5% defatted milk. Thereafter, the membranes were washed with TBS-T buffer and incubated for 45 min with anti-rabbit IgG Horseradish Peroxidase (HRP) conjugated secondary antibody (ab6721 Abcam, Cambridge, UK 1:5000 dilution). After washing, immunoreactive protein was visualised using an enhanced chemoluminescence-based detection kit, following the manufacturer's protocol (Thermo Scientific Pierce ECL Plus Western Blotting Substrate) and a CCD Camera (G-Box, Syngene, Cambridge, UK) gel system. Scanned blots were analysed using GensSnap software (Syngene, Cambridge, UK) and dot densities were expressed as a percentage of those taken from the control cultures. The statistical analysis was performed as described above.

5.18. ELISA for Aβ

In order to detect Aβ secreted by PC12 cells, an Aβ42 ELISA kit (provided by Invitrogen Corporation Camarillo, CA 93012 Catalog #: KMB3441) technique was used. The ELISA procedure was as follows: after 1 h of treatment, the culture medium was collected and diluted to 1:100, using culture medium as diluent. Four repeats of each diluted sample were then placed in the Aβ42 capture antibody pre-coated wells. The detection was then carried out following the manufacturer's protocol. Briefly, the samples were incubated for 4 h in presence of 50 μl of detection antibody. The plate was then washed seven times with the washing solution, the samples were then incubated with the 3,3′,5,5′-tetramethylbenzidine (TMB) provided with the kit for 15 min after the sample revelation the reaction was stopped with the stop solution and the optical density was read at 450 nm.

5.19. Drugs and reagents

MEM, culture serums, antibiotics, collagen, Cell Counting Kit-8 and buffers reagents were provided by Sigma–Aldrich (St. Louis, MO). [^{3}H] Ivermectin was purchased from American Radiolabeled chemicals (USA). T30, T14 (C-terminal W), T14 (C-terminal K) and NBP14 were synthesised by Genosphere Biotechnologies (France). Aβ and Fluo-8 were provided by Abcam (Cambridge, UK). Galantamine was provided by Tocris. AChE was provided by Worthington Biochemical Corp (New Jersey, USA).

5.20. Data analysis

In each of the different PC12 cell techniques, the statistics analysis was performed with the average of the percentage values of 3 or more experiments. Comparisons between multiple treatment groups and the same control were performed by one-way analysis of variance (ANOVA) and Tukey's post-hoc tests using GraphPAD Instat (GraphPAD software, San Diego, CA). Statistical significance was taken at a p value < 0.05. In the case of the binding experiment, results were obtained as counts per minute (cpm) and transformed to percentages related to control. Results were fitted to a model of one site competition binding using GraphPad Prism (GraphPAD software, San Diego, CA). The EC50 values were calculated by fitting the logarithm of the experimental data points to a single site Hill equation using a non-linear regression curve using GraphPad Prism. For the human brain experiments, the analysis of data was represented in the figures as the average of the values of 5 control and 7 Alzheimer's patients. In order to convert optical density readings to molarity in each sample, a calibration curve was used where different, known concentrations of T14 were plotted against the respective reading using an ‘exponential model’. Finally values were standardised as content of T14 related to total protein (μg/mg). For the Aβ ELISA data, outliers were designated by the modified Thompson Tau method, resulting in the removal of one data point from the control group.

Author contributions

SG-R: Responsible for data shown in Figs. 2–4, Table 1 and drawing Fig 5, plus assistance with MS preparation/writing.

PM: Responsible for data shown in Fig. 1b, d and 2c.

HT: Responsible for data shown in Fig 1e.

GP: Assistance with initial characterisation of antibody and specification for cyclisation of peptide T14. Responsible for Fig. 3a and b.

A-SB: Dissection and preparation of human brain tissue.

CTG: Assistance with experiments described in Figs. 2–4.

CH: Assistance with experiments described in Figs. 2–4.

CWC: Assistance with writing MS.

SAG: Responsible for original basic concepts, planning overall programme, and writing MS.

Author information

SAG is a Senior Research Fellow, Lincoln College Oxford.

The authors declare competing financial interests. Susan Greenfield is the founder and CEO of Neuro-Bio Limited and holds shares in the Company. Sara Garcia-Ratés, Paul Morrill, Henry Tu and Antoine-Scott Badin are employees of Neuro-Bio Ltd. Gwenael Pottiez, Cristina Tormo-Garcia and Catherine Heffner (who have now left the company) were full-time researchers with Neuro-Bio: GP was a post-doc, CT-G and CH were interns.

Clive Coen is Professor of Neuroscience at King's College London.

Correspondence and requests for materials should be addressed

to Sara Garcia-Ratés: sara.garciarates@neuro-bio.com.

Acknowledgements

The work described in this paper is covered by patent applications, WO 2015/004430 and GB1505239.2. We would also like to thank the following for their comments: Dr Linda Cammish (Neuro-Bio Ltd), Dr Colin Masters (Melbourne University), Mr Charlie Morgan (Neuro-Bio Ltd), Dr Rod Porter (Porter Consultancy), Professor John Stein (Oxford University), Mr Martin Westwell (Flinders University).

We are grateful to Professor Margaret Esiri (John Radcliffe Hospital) for supplying the image in Fig. 1C. as well as the brain tissue samples, in addition to commenting on the MS and to Dr Robin Murphy (Dept Psychology Oxford) for his help with the statistical analysis of the human brain samples.

References

Albanese, A., Butcher, L.L., 1980. Acetylcholinesterase and catecholamine distribution in the locus ceruleus of the rat. Brain Res. Bull. 5 (2), 127–134.
Aletrino, M.A., Vogels, O.J., Van Domburg, P.H., Ten Donkelaar, H.J., 1992. Cell loss in the nucleus raphes dorsalis in Alzheimer's disease. Neurobiol. Aging 13 (4), 461–468.
Appleyard, M.E., McDonald, B., 1991. Reduced adrenal gland acetylcholinesterase activity in Alzheimer's disease. Lancet 338 (8774), 1085–1086.
Arendt, T., Bruckner, M.K., Lange, M., Bigl, V., 1992. Changes in acetylcholinesterase and butyrylcholinesterase in Alzheimer's disease resemble embryonic development–a study of molecular forms. Neurochem. Int. 21 (3), 381–396.
Badin, A.S., Eraifej, J., Greenfield, S., 2013. High-resolution spatio-temporal bioactivity of a novel peptide revealed by optical imaging in rat orbitofrontal cortex in vitro: possible implications for neurodegenerative diseases. Neuropharmacology 73, 10–18.
Badin, A.S., Morrill, P., Devonshire, I., Greenfield, S.A., 2016 Jan 7. (II) Physiological profiling of an endogenous acetylcholinesterase-derived peptide in the basal forebrain: age-related bioactivity and blockade with a novel modulator. Neuropharmacology. 105, 47–60. http://dx.doi.org/10.1016/j.neuropharm.2016.01.012 [Epub ahead of print].
Bon, C.L., Greenfield, S.A., 2003. Bioactivity of a peptide derived from acetylcholinesterase: electrophysiological characterization in guinea-pig hippocampus. Eur. J. Neurosci. 17 (9), 1991–1995.
Bond, C.E., Zimmermann, M., Greenfield, S.A., 2009. Upregulation of alpha7 nicotinic receptors by acetylcholinesterase c-terminal peptides. PLoS One 4 (3), e4846.
Bornstein, S.R., Ehrhart-Bornstein, M., Androutsellis-Theotokis, A., Eisenhofer, G., Vukicevic, V., Licinio, J., Wong, M.L., Calissano, P., Nistico, G., Preziosi, P., Levi-Montalcini, R., 2012. Chromaffin cells: the peripheral brain. Mol. Psychiatry 17 (4), 354–358.
Braak, H., Del Tredici, K., 2011. Alzheimer's pathogenesis: is there neuron-to-neuron propagation? Acta Neuropathol. 121 (5), 589–595.
Broide, R.S., Robertson, R.T., Leslie, F.M., 1996. Regulation of alpha7 nicotinic acetylcholine receptors in the developing rat somatosensory cortex by thalamocortical afferents. J. Neurosci. 16 (9), 2956–2971.
Card, J.P., Meade, R.P., Davis, L.G., 1988. Immunocytochemical localization of the precursor protein for beta-amyloid in the rat central nervous system. Neuron 1 (9), 835–846.
Chu, L.W., Ma, E.S., Lam, K.K., Chan, M.F., Lee, D.H., 2005. "Increased alpha 7 nicotinic acetylcholine receptor protein levels in Alzheimer's disease patients. Dement. Geriatr. Cogn. Disord. 19 (2–3), 106–112.
Collins, M.A., An, J., Peller, D., Bowser, R., 2015. Total protein is an effective loading control for cerebrospinal fluid Western blots. J. Neurosci. Meth. 251, 72–82.
Cottingham, M.G., Hollinshead, M.S., Vaux, D.J., 2002. "Amyloid fibril formation by a synthetic peptide from a region of human acetylcholinesterase that is homologous to the Alzheimer's amyloid-beta peptide. Biochem. 41, 13539–13547.
Coyle, J., Kershaw, P., 2001. Galantamine, a cholinesterase inhibitor that allosterically modulates nicotinic receptors: effects on the course of Alzheimer's disease. Biol. Psychiatry 49 (3), 289–299.
Darvesh, S., 2013. Butyrylcholinesterase radioligands to image Alzheimer's disease brain. Chem. Biol. Interact. 203 (1), 354–357.
Day, T., Greenfield, S.A., 2004. Bioactivity of a peptide derived from acetylcholinesterase in hippocampal organotypic cultures. Exp. Brain Res. 155 (4), 500–508.
Dickie, B.G., Holmes, C., Greenfield, S.A., 1996. Neurotoxic and neurotrophic effects of chronic N-methyl-D-aspartate exposure upon mesencephalic dopaminergic neurons in organotypic culture. Neuroscience 72 (3), 731–741.
Dickinson, J.A., Hanrott, K.E., Mok, M.H., Kew, J.N., Wonnacott, S., 2007. Differential coupling of alpha7 and non-alpha7 nicotinic acetylcholine receptors to calcium-induced calcium release and voltage-operated calcium channels in PC12 cells. J. Neurochem. 100 (4), 1089–1096.
Eckert, G.P., Wood, W.G., Muller, W.E., 2005. Membrane disordering effects of beta-amyloid peptides. Subcell. Biochem. 38, 319–337.
Eimerl, S., Schramm, M., 1994. The quantity of calcium that appears to induce neuronal death. J. Neurochem. 62 (3), 1223–1226.
Garcia-Ayllón, M.-S., Llorens, E., Avila, J., Alom, J., Saez-Valero, J., 2014. Elevated acetylcholinesterase levels by hyperphosphorylated tau overexpression. Alzheimer's Dementia 10 (4), P651.
Garcia-Ayllon, M.S., Riba-Llena, I., Serra-Basante, C., Alom, J., Boopathy, R., Saez-Valero, J., 2010. Altered levels of acetylcholinesterase in Alzheimer plasma. PLoS One 5 (1), e8701.
Garcia-Ayllon, M.S., Small, D.H., Avila, J., Saez-Valero, J., 2011. Revisiting the role of acetylcholinesterase in Alzheimer's disease: cross-talk with p-tau and beta-amyloid. Front. Mol. Neurosci. 4, 22.
Garcia-Rates, S., Lewis, M., Worrall, R., Greenfield, S.A., 2013. Additive toxicity of beta-amyloid by a novel bioactive peptide in vitro: possible implications for Alzheimer's disease. PLoS One 8 (2), e54864.
Gendron, T.F., Petrucelli, L., 2009. The role of tau in neurodegeneration. Mol. Neurodegener. 4, 13.
Giacobini, E., Gold, G., 2013. "Alzheimer disease therapy–moving from amyloid-beta to tau. Nat. Rev. Neurol. 9 (12), 677–686.
Gilon, C., Halle, D., Chorev, M., Selinger, Z., Byk, G., 1991. Backbone cyclization: a new method for conferring conformational constraint on peptides. Biopolymers 31 (6), 745–750.
Goodwin, D., Simerska, P., Toth, I., 2012. Peptides as therapeutics with enhanced bioactivity. Curr. Med. Chem. 19 (26), 4451–4461.
Greene, L.A., Tischler, A.S., 1976. Establishment of a noradrenergic clonal line of rat adrenal pheochromocytoma cells which respond to nerve growth factor. Proc. Natl. Acad. Sci. U. S. A. 73 (7), 2424–2428.
Greenfield, S., 2013. Discovering and targeting the basic mechanism of neurodegeneration: the role of peptides from the C-terminus of acetylcholinesterase: non-hydrolytic effects of ache: the actions of peptides derived from the C-terminal and their relevance to neurodegeneration. Chem. Biol. Interact. 203 (3), 543–546.
Greenfield, S.A., Day, T., Mann, E.O., Bermudez, I., 2004. A novel peptide modulates alpha7 nicotinic receptor responses: implications for a possible trophic-toxic mechanism within the brain. J. Neurochem. 90 (2), 325–331.
Hartigan, J.A., Johnson, G.V., 1999. Transient increases in intracellular calcium result in prolonged site-selective increases in Tau phosphorylation through a glycogen synthase kinase 3beta-dependent pathway. J. Biol. Chem. 274 (30), 21395–21401.
Haworth, D., Rees, A., Alcock, P.J., Wood, L.J., Dutta, A.S., Gormley, J.J., Jones, H.B., Jamieson, A., Reilly, C.F., 1999. Anti-inflammatory activity of c(ILDV-NH(CH2)5CO), a novel, selective, cyclic peptide inhibitor of VLA-4-mediated cell adhesion. Br. J. Pharmacol. 126 (8), 1751–1760.
He, G., Luo, W., Li, P., Remmers, C., Netzer, W.J., Hendrick, J., Bettayeb, K., Flajolet, M., Gorelick, F., Wennogle, L.P., Greengard, P., 2010. Gamma-secretase activating protein is a therapeutic target for Alzheimer's disease. Nature 467 (7311), 95–98.
Horvath, J., Burkhard, P.R., Herrmann, F.R., Bouras, C., Kovari, E., 2014. Neuropathology of parkinsonism in patients with pure Alzheimer's disease. J. Alzheimers Dis. 39 (1), 115–120.
Howell, S.M., Fiacco, S.V., Takahashi, T.T., Jalali-Yazdi, F., Millward, S.W., Hu, B., Wang, P., Roberts, R.W., 2014. Serum stable natural peptides designed by mRNA display. Sci. Rep. 4, 6008.
Irwin, D.J., Lee, V.M., Trojanowski, J.Q., 2013. Parkinson's disease dementia: convergence of alpha-synuclein, tau and amyloid-beta pathologies. Nat. Rev. Neurosci. 14 (9), 626–636.
Lamberto, I., Lechtenberg, B.C., Olson, E.J., Mace, P.D., Dawson, P.E., Riedl, S.J., Pasquale, E.B., 2014. Development and structural analysis of a nanomolar cyclic peptide antagonist for the EphA4 receptor. ACS Chem. Biol. 9 (12), 2787–2795.
Laferla, F.M., Green, K.N., 2012. Animal models of Alzheimer disease. Cold Spring Harb. Perspect. Med. 2 (11) pii: a006320.
Laurijssens, B., Aujard, F., Rahman, A., 2013. Animal models of Alzheimer's disease and drug development. Drug Discov. Today Technol. 10, e319–e327.
Ludwig J., Rabe H., Höffle-Maas A., Samochocki M., Maelicke A. and Kaletta T. Directed mutagenesis of nicotinic receptors to investigate receptor function. Biochem. Genet. Mol. Biol., "Genetic Manipulation of DNA and Protein – Examples from Current Research", book edited by David Figurski, ISBN 978-953-51-0994-5, Published: February 5, 2013 under CC BY 3.0 license.
Mondragon-Rodriguez, S., Perry, G., Zhu, X., Boehm, J., 2012. Amyloid Beta and tau proteins as therapeutic targets for Alzheimer's disease treatment: rethinking the current strategy. Int. J. Alzheimers Dis. 2012, 630182.
Morris, G.P., Clark, I.A., Vissel, B., 2014. Inconsistencies and controversies surrounding the amyloid hypothesis of Alzheimer's disease. Acta Neuropathol. Commun. 2, 135.
Nagele, R.G., D'Andrea, M.R., Anderson, W.J., Wang, H.Y., 2002. Intracellular accumulation of beta-amyloid(1-42) in neurons is facilitated by the alpha 7 nicotinic acetylcholine receptor in Alzheimer's disease. Neuroscience 110 (2), 199–211.
Nery, A.A., Resende, R.R., Martins, A.H., Trujillo, C.A., Eterovic, V.A., Ulrich, H., 2010. Alpha7 Nicotinic acetylcholine receptor expression and activity during neuronal differentiation of PC12 pheochromocytoma cells. J. Mol. Neurosci. 41, 329–339.
Ni, R., Marutle, A., Nordberg, A., 2013. Modulation of alpha7 nicotinic acetylcholine receptor and fibrillar amyloid-beta interactions in Alzheimer's disease brain. J. Alzheimers Dis. 33 (3), 841–851.
Rogers, S.W., Mandelzys, A., Deneris, E.S., Cooper, E., Heinemann, S., 1992. The expression of nicotinic acetylcholine receptors by PC12 cells treated with NGF.

J. Neurosci. 12, 4611–4623.
Rossor, M.N., 1981. Parkinson's disease and Alzheimer's disease as disorders of the isodendritic core. Br. Med. J. Clin. Res. Ed. 283 (6306), 1588–1590.
Saez-Valero, J., Fodero, L.R., White, A.R., Barrow, C.J., Small, D.H., 2003. Acetylcholinesterase is increased in mouse neuronal and astrocyte cultures after treatment with beta-amyloid peptides. Brain Res. 965 (1–2), 283–286.
Samochocki, M., Zerlin, M., Jostock, R., Groot Kormelink, P.J., Luyten, W.H., Albuquerque, E.X., Maelicke, A., 2000. Galantamine is an allosterically potentiating ligand of the human alpha4/beta2 nAChR. Acta Neurol. Scand. Suppl. 176, 68–73.
Seguela, P., Wadiche, J., Dineley-Miller, K., Dani, J.A., Patrick, J.W., 1993. Molecular cloning, functional properties, and distribution of rat brain alpha 7: a nicotinic cation channel highly permeable to calcium. J. Neurosci. 13 (2), 596–604.
Svedberg, M.M., Svensson, A.L., Johnson, M., Lee, M., Cohen, O., Court, J., Soreq, H., Perry, E., Nordberg, A., 2002. Upregulation of neuronal nicotinic receptor subunits alpha4, beta2, and alpha7 in transgenic mice overexpressing human acetylcholinesterase. J. Mol. Neurosci. 18 (3), 211–222.
Takeda, M., Tanaka, S., Kido, H., Daikoku, S., Oka, M., Sakai, K., Katunuma, N., 1994. Chromaffin cells express Alzheimer amyloid precursor protein in the same manner as brain cells. Neurosci. Lett. 168 (1–2), 57–60.
Wang, H.Y., Lee, D.H., Davis, C.B., Shank, R.P., 2000. Amyloid peptide Abeta(1-42) binds selectively and with picomolar affinity to alpha7 nicotinic acetylcholine receptors. J. Neurochem. 75 (3), 1155–1161.
Woolf, N.J., 1996. Global and serial neurons form A hierarchically arranged interface proposed to underlie memory and cognition. Neuroscience 74 (3), 625–651.